35th Annual International Conference of the IEEE EMBS
Osaka, Japan, 3 - 7 July, 2013

An experimental protocol for the definition of upper limb anatomical frames on children using magneto–inertial sensors

L. Ricci, *Student Member, IEEE*, D. Formica, *Member, IEEE*, E. Tamilia, *Student Member, IEEE*, F. Taffoni, *Member, IEEE*, L. Sparaci, O. Capirci, E. Guglielmelli, *Senior Member, IEEE*

***Abstract*— Motion capture based on magneto-inertial sensors is a technology enabling data collection in unstructured environments, allowing "out of the lab" motion analysis. This technology is a good candidate for motion analysis of children thanks to the reduced weight and size as well as the use of wireless communication that has improved its wearability and reduced its obtrusivity. A key issue in the application of such technology for motion analysis is its calibration, i.e. a process that allows mapping orientation information from each sensor to a physiological reference frame. To date, even if there are several calibration procedures available for adults, no specific calibration procedures have been developed for children. This work addresses this specific issue presenting a calibration procedure for motion capture of thorax and upper limbs on healthy children. Reported results suggest comparable performance with similar studies on adults and emphasize some critical issues, opening the way to further improvements.**

I. Introduction

The advent of MEMS technology in the 90s has fostered the development of wearable sensors for measuring kinematic, dynamic and even tribological [1], [2] quantities. An outstanding example of this trend are Magnetic and Inertial Measurement Unit (M-IMU) sensors, which identify a class of devices comprising accelerometers, gyroscopes and magnetometers.Besides acceleration, magnetic field and angular velocity, the information coming from this kind of sensor is usually combined to get an estimate of orientation, relative to a global, earth-based System of Reference (SoR). To this aim, a broad range of data fusion algorithms have been explored in the literature [3], [4]; the most widespread techniques are adaptations of the Extended Kalman Filter (EKF) or its complementary version [5].

A small size board equipping a M-IMU, a microcontroller, a wireless communication and/or a micro SD memory for data logging, is nowadays a well established approach to the 3D human motion sensing and reconstruction problem [6]. The main drawbacks of this technology are drift issues that affect orientation estimate, which are mostly due to gyroscopes integration and to the alteration of calibration parameters. Furthermore, exposure to strong magnetic fields may affect sensor performance, therefore periodic spot–checks are required in order to re–assess system calibration [7].

Nonetheless, compared to other available motion tracking technologies, magneto–inertial sensors appear to be the "closest thing to a silver bullet" for motion analysis on children [8], [9], [10]. The possibility to precisely track and quantitatively analyze children's motion repertoire is of great interest for a number of reasons. In fact, motor actions play an important role during social interactions, as proven by recent findings on *mirror* functions of the motor system [11]. Furthermore, studies on motor and communicative actions (e.g. gestures) in children with autistic spectrum disorder (ASD) have highlighted the importance of assessing motor behaviours for early diagnosis and intervention[12]. Tools usually employed in the analysis of human motor control often require cumbersome machineries and dedicated experimental settings and laboratories [13], [14]. Therefore the development of appropriate evaluation tools usable in unstructured environments may be of relevance in research on both typical and atypical development.

Effective use of M-IMU sensors for human motion analysis requires: *(i)* the determination of the most appropriate body areas where each sensor should be attached; *(ii)* dedicated calibration procedures to assign to each body segment an anatomical frame of reference (AF), and to define the transformations between AFs and sensors' reference frames.

Gold standard procedure to define local SoR would require measurements of bony landmarks [15]. However, this can not be applied to *"in-field"* applications. Therefore, other procedures have been proposed for "in field" calibration, which proved to be successful both for upper and lower limbs [16], [17], [18], [19], [20]. In fact, there are two possible techniques for the definition of local SoR using M-IMU sensors: reference and/or functional method.

In the reference method, the subject wearing the M-IMUs is asked to hold a certain established body configuration (e.g. the standard anatomical position (SAP)).

On the contrary, functional methods are based on subjects performing mono–axial movements. In this second case, choice of movements to be performed is crucial for the reliability of the estimated SoR.

Notwithstanding the existence of various studies documenting efficient calibration procedures for adults, no study to date provides an efficient method to calibrate a magneto-inertial tracking system for its use with children.

The main goal of this paper is to provide novel data on defining and implementing a calibration protocol to define

Manuscript received February 4, 2013. This work was partly funded by the Italian Ministry of Education, University and Research under the FIRB "Futuro in Ricerca" research program (TOUM project, no. RBFR086HEW). Luca Ricci, Domenico Formica, Eleonora Tamilia and Eugenio Guglielmelli are with the Laboratory of Biomedical Robotics and Biomicrosystems, Università Campus Bio-Medico di Roma, Via Alvaro del Portillo, 21, 00128, Rome, Italy (e-mail: {l.ricci; d.formica; e.tamilia; f.taffoni; e.guglielmelli}@unicampus.it). Laura Sparaci and Olga Capirci are with the Institute of Cognitive Sciences and Technologies, CNR, Via Nomentana 56, 00161, Rome, Italy

local SoR for thorax and upper limbs, usable with healthy, tipically developing (TD) children. In the following, the proposed methodology is described in details and the preliminary results are reported.

II. Materials and Methods

A. Experimental setup

A set of 5 sensor units (Opal by APDM Inc.) were wirelessly connected to a PC via an "access point" transceiver provided by the manufacturer. Each sensor is a lightweight box (22 g) containing a M-IMU and a micro SD for robust sensor data logging. The orientation information of the global, earth-based SoR (G) with respect to the sensor local SoR (S) is also available via the manufacturer Kalman filter, in the form of a quaternion q_S^G. The orientation estimate is claimed to have a static and a dynamic accuracy of $\sim 1.5°$ RMS and $\sim 2.8°$, respectively.

We developed a custom software platform, written in C++ using the manufacturer API, for synchronized data collection at the maximum update rate of 128 Hz. The software is also provided with tools for real–time data plotting and 3D motion visualization via a virtual reality (VR) environment; the VR environment embeds a simple kinematic model of a 3D character, which and has been developed using the OGRE framework.

In our application, we considered thorax, upper arm, and forearm as rigid segments, that constitute the kinematic chain of the upper limbs.

A ball-in-a-socket type is assumed for all the joints of interest, i.e. any possible rotation in the $SO(3)$ space is admitted. No model constraints (e.g. the elbow ab-adduction) have been implemented at this stage, since the goal of this work is to evaluate the performance of the proposed calibration procedure.

Previously to data acquisition, accelerometer and magnetometer calibration was assessed with the "in field" methodology proposed in [9] and the gyroscope offset was checked to be well under 0.1 rad/s, as suggested by the manufacturer.

B. Methodology description

The 5 sensor units were placed on: thorax, latero-distally on the right and left upper–arm, and near the wrist on the right and left forearm. Each sensor was fixed on the body segment of interest using the Velcro straps, provided by the sensors' manufacturer. Being each body segment and its connection to the respective sensor assumed as rigid, a coordinate transformation between each sensor SoR and its relative body segment SoR can be described by a matrix in the $SO(3)$. In order to estimate these rotation matrices, that map each sensor SoR to the one of the relative body segment a calibration protocol, involving both reference and functional methodologies, was deployed.

For the reference part of the protocol, each subject was asked to stand up, with arms close to the body and elbows flexed at $90°$ for about 5 seconds. 3 separate acquisitions were recorded with subjects in the same posture. The measured gravity vector has been normalized and averaged over the 3 trials, in order to estimate vertical axis of reference. Since magnetic measurements are affected by "soft iron" errors, no reference axis from magnetic vector was considered.

For the functional part of the protocol, a set of mono-

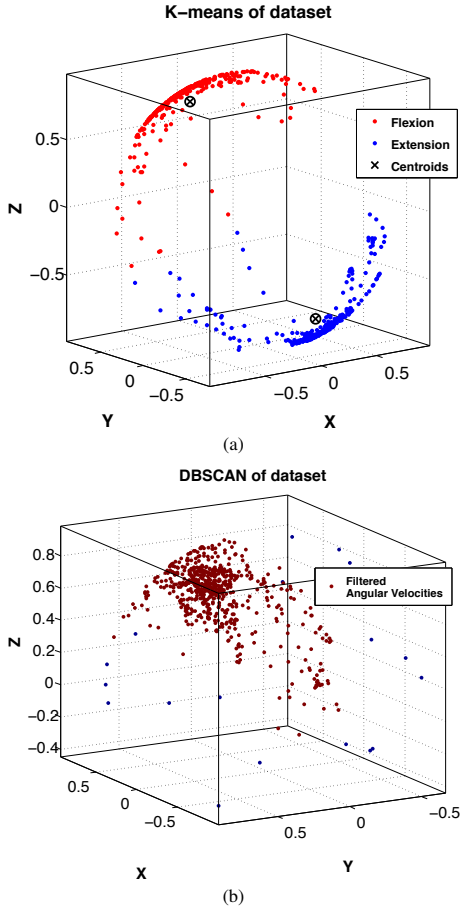

Fig. 1. Normalized angular velocity vectors: in *(a)* segmentation of upper arm movement via *k*–means clustering algorithm. The algorithm allows to distinguish between the flexion and extension movement; in *(b)* the filtering of noise and outlayers performed by the DBSCAN algorithm is reported, the brown dots are the filtered angular velocities.

axial movements was defined to determine axes of rotation. Each movement is composed by two opposite rotations. The whole sequence of the movements performed by each subject is reported in the following:

- Thorax
  - forward flexion–extension to $\sim 45°$
  - lateral ab–adduction
- Upper arm
  - arm forward flexion–extension while holding a light rod at shoulder breadth
  - ab–adduction to $\sim 60°$
- Forearm
  - flexion–extension while holding a light rod at shoulder breadth and upper arms close to the body
  - prono–supination with elbow flexed at $90°$

For each movement a total of 3 repetitions (trial) was performed; the subject was requested to repeat the whole sequence 3 times. During the movements angular velocities were continuously recorded and precessed in the following steps in order to extract a functional axis of rotation. First of all, data were filtered with a two-way, 4^{th} order, lowpass Butterworth filter with 10 Hz cut–off frequency, to reduce higher frequency noise (a preliminary analysis of power spectral density indicated that signal information is mainly concentrated in the 0-1 Hz range).

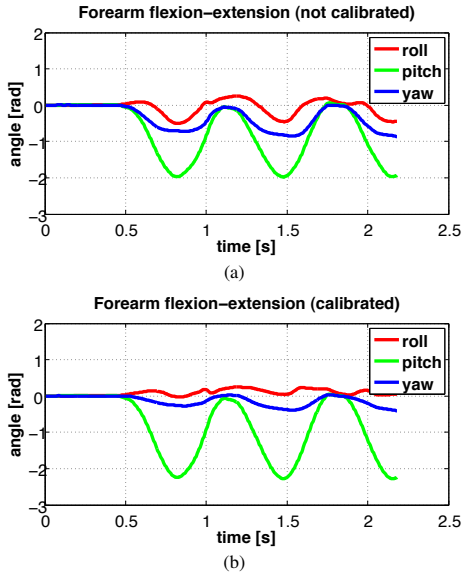

Fig. 2. Orientation angles, expressed as Euler roll–pitch–yaw, respectively for the uncalibrated (a) and calibrated (b) movements.

The second step was implemented in order to enable a clear segmentation of actions (e.g. separate flexion from extension movement or pronation from supination); a lower threshold equal to 5% of peak angular velocity was set to detect the onset and end of each movement. Then, the resulting data were normalized and segmented by means of a *k*–means data clustering algorithm, assuming that only two clusters have to be found in the dataset (i.e. the pair of rotations with the same axis and opposite in sign that compose the movement).

Thorax	**Children (N = 4)**	**Adults (N = 4)**
gravity	1.25 ± 0.62	0.41 ± 0.15
flexion–extension	1.89 ± 0.87	1.37 ± 0.23
lateral–flexion	6.11 ± 1.96	2.49 ± 1.02
Upper am	**Children (N = 4)**	**Adults (N = 4)**
gravity	3.07 ± 2.03	0.35 ± 0.06
flexion–extension	4.92 ± 2.05	1.84 ± 0.48
ab-adduction	3.96 ± 0.97	2.46 ± 0.79
Forearm	**Children (N = 4)**	**Adults (N = 4)**
gravity	9.90 ± 5.94	0.49 ± 0.22
flexion–extension	2.52 ± 0.82	1.53 ± 0.67
prono–supination	3.37 ± 2.81	1.07 ± 0.79

TABLE I

ANGULAR DISPERSION (ε) OF EACH MOVEMENT EXPRESSED AS THE MEAN VALUE OVER THE TRIALS $\pm$ SD.

The whole dataset of normalized angular velocities is distributed over the surface of an unitary radius sphere in $\mathbb{R}^3$ (see Fig. 1 a). Finally, to further remove outliers and noise, the pair of identified clusters is mapped on the same hemisphere (by changing the direction of the vectors composing one of the two clusters). This allows to apply a density–based clustering algorithm, namely DBSCAN which filters out noise and outliers by detecting clusters of arbitrary shapes based on the definition of *density–reachability* (see Fig. 1 b, for further details refers to [21]). The typical output of the two clustering operations is shown in Fig. 1. The functional axis was extracted from the processed data as the averaged, normalized angular velocity vector.

For each estimated axis, a measure of the dispersion (ε) proposed by [18] was evaluated as:

$$\varepsilon = \frac{\sum_{i=1}^{3} arccos(\vec{v}_i \cdot \vec{v}_{avg})}{3} \quad (1)$$

where $\vec{v}_{avg}$ is the average axis of the whole trial set and $\vec{v}_i$ is the average axis computed on a single trial.

The output of the proposed calibration procedure is a set of 3 axes for each body segment, one from the reference and the other from the functional part. In order to estimate the 3D rotation matrix between the sensor SoR and the corresponding AF, only a couple of non-aligned axes is needed. The whole set of estimated axes was ranked by the dispersion parameter and the couple exhibiting the lowest ones was selected. For example, being $(\vec{a}_1, \vec{a}_2)$ the vector pair, with $\varepsilon(\vec{a}_1) < \varepsilon(\vec{a}_2)$, the SO(3) matrix relating the sensor SoR to the corresponding body segment AF can be defined as:

$$R = [\vec{a_1}, (\vec{a_1} \times \vec{a_2}) \times \vec{a_1}, \vec{a_1} \times \vec{a_2}] \quad (2)$$

III. RESULTS

Proposed methodology was tested on a group of four healthy TD children (age 7 $\pm$ 0.3 years) who participated in this study. All parents have provided written consent. To better evaluate method performance in relation to existing literature, an equal number of adult subjects (age 27 $\pm$ 1.9 years) was tested.

The whole protocol was presented to the child as an imitation task. Therefore, procedure required the presence of an adult standing in front of the child and requesting the child to mirror adult movements. Particular care was taken to limit overall protocol duration to less than 5 minutes, including M-IMU sensor wearing time and system start-up.

The results of the experimentation are reported in table I. Dispersion values were on average quite low for adults and acceptable for children, compared to data in literature [18]. Particularly, dispersion values in adults and in children resulted significantly different ($p < 0.05$), except for the thorax flexion-extension movement. A two-tailed *t*–test or Wilcoxon's rank–sum test were used as appropriate.

In particular, the choice of a reference position with the elbow flexed at 90° has proved to be unsuitable for children experiment. In fact, in most cases they tried to continuously

correct the arm configuration in order to imitate the adult, rather than keeping a fixed position. Moreover, an unwanted prono–supination component during the flexion–extension movement of the forearm and upper arm has been shown to be more evident in children than adults. This artifact is probably due to the presence of a light rod used to constraint the lateral sway.

Despite a rigorous validation of the protocol (using a stereophotogrammetric system) has not been carried out, a preliminary indication about the correctness of the estimated axes was obtained by the analysis of the M-IMUs orientation measurements; after the calibration matrices are obtained using the aforementioned methodology, we refer acquired quaternion data (q_S^G), originally expressed in the sensor SoR, into the corresponding AF (q_{AF}^G). Since functional movements were selected conforming with the mono–axiality hypothesis, a quasi–monoaxial movement should be observed from the calibrated data.

Both orientation angles expressed in AF and in the sensor SoR, expressed as roll–pitch–yaw angles are shown in fig. 2, for the case of forearm flexion–extension movement. The orientation data appear to confirm the mono–axiality hypothesis as expected.

IV. Conclusions

A methodology for the assignment of AFs to the upper extremity using a magneto–inertial motion tracking system on children has been proposed. By choosing the axes with the lowest dispersion, a 3D rotation matrix can be estimated and used to relate orientation information from the sensors to the physiological motion. Moreover, through a mathematical model of the human body, the described procedure enables the reconstruction of the upper limb kinematics in children using M-IMU measurement (e.g. see the VR environment in Fig. 3.

Finally, critical issues relating to the choice of calibration movements, which has been proved to be appropriate in adults but ineffective in children, have been emphasized, suggesting future improvements of the protocol, to allow its use in children with typical and atypical development.

References

[1] D. Accoto, R. Sahai, F. Damiani, D. Campolo, E. Guglielmelli, and P. Dario, "A slip sensor for biorobotic applications using a hot wire anemometry approach," *Sensors and Actuators, A: Physical*, vol. 187, pp. 201–208, 2012.

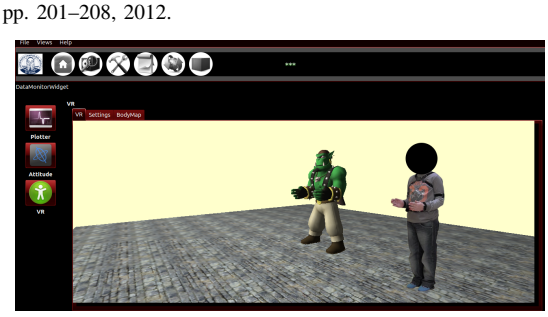

Fig. 3. A screenshot of the C++ Virtual Reality platform used for children motion analysis and reconstruction.

[2] M. Francomano, D. Accoto, E. Morganti, L. Lorenzelli, and E. Guglielmelli, "A microfabricated flexible slip sensor," *Proceedings of the IEEE RAS and EMBS International Conference on Biomedical Robotics and Biomechatronics (BIOROB2012)*, pp. 1919–1924, 2012.

[3] R. Mahony, S. Member, T. Hamel, and J. M. Pflimlin, "Nonlinear Complementary Filters on the Special Orthogonal Group," *IEEE Transactions on Automatic Control*, vol. 53, pp. 1203–1218, Jun. 2008.

[4] S. O. H. Madgwick, A. J. L. Harrison, and A. Vaidyanathan, "Estimation of IMU and MARG orientation using a gradient descent algorithm.," *IEEE International Conference on Rehabilitation Robotics*, pp. 1–7, Jun. 2011.

[5] J. Crassidis, F. L. Markley, and Y. Cheng, "A Survey of Nonlinear Attitude Estimation Methods," *AIAA Journal of Guidance, Control, and Dynamics*, vol. 30, no. 1, pp. 12–28, 2007.

[6] H. Harms, O. Amft, R. Winkler, J. Schumm, M. Kusserow, and G. Troester, "ETHOS: Miniature orientation sensor for wearable human motion analysis," *IEEE Sensors*, pp. 1037–1042, Nov. 2010.

[7] P. Picerno, A. Cereatti, and A. Cappozzo, "A spot check for assessing static orientation consistency of inertial and magnetic sensing units," *Gait & Posture*, vol. 33, pp. 373–378, Mar. 2011.

[8] G. Welch and E. Foxlin, "Motion Tracking: No Silver Bullet, but a Respectable Arsenal," *IEEE Computer Graphics and Applications*, pp. 24–38, Dec. 2002.

[9] D. Campolo, F. Taffoni, D. Formica, G. Schiavone, F. Keller, and E. Guglielmelli, "Inertial-Magnetic Sensors for Assessing Spatial Cognition in Infants," *IEEE Transaction on Biomedical Engineering*, vol. 58, pp. 1499–1503, May. 2011.

[10] F. Taffoni, V. Focaroli, D. Formica, E. Gugliemelli, F. Keller, and J. M. Iverson, "Sensor-based technology in the study of motor skills in infants at risk for ASD," *2012 4th IEEE RAS & EMBS International Conference on Biomedical Robotics and Biomechatronics (BioRob)*, pp. 1879–1883, Jun. 2012.

[11] G. Rizzolatti and C. Sinigaglia, "The functional role of the parieto-frontal mirror circuit: interpretations and misinterpretations," *Nature Reviews Neuroscience*, vol. 38, pp. 264–274, Apr. 2010.

[12] C. von Hofsten and K. Rosander, "Perception-action in children with ASD," *Frontiers in Integrative Neuroscience*, vol. 6, pp. 1–6, Dec. 2012.

[13] D. Formica, S. Charles, L. Zollo, E. Guglielmelli, N. Hogan, and K. HI, "The passive stiffness of the wrist and forearm," *Journal of Neurophysiology*, vol. 108, no. 4, pp. 1158–1166, 2012.

[14] G. Pellegrino, M. Tombini, G. Assenza, M. Bravi, S. Sterzi, V. Giacobbe, L. Zollo, E. Guglielmelli, G. Cavallo, F. Vernieri, and F. Tecchio, "Inter-hemispheric coupling changes associate with motor improvements after robotic stroke rehabilitation," *Restorative Neurology and Neuroscience*, vol. 30, no. 6, pp. 497–510, 2012.

[15] G. Wu, F. C. van der Helm, H. (DirkJan) Veeger, M. Makhsous, P. Van Roy, C. Anglin, J. Nagels, A. R. Karduna, K. McQuade, X. Wang, F. W. Werner, and B. Buchholz, "ISB recommendation on definitions of joint coordinate systems of various joints for the reporting of human joint motion—Part II: shoulder, elbow, wrist and hand," *Journal of Biomechanics*, vol. 38, pp. 981–992, May. 2005.

[16] F. Taffoni, G. Piervirgili, D. Formica, and E. Guglielmelli, "An alignment procedure for ambulatory measurements of lower limb kinematic using magneto-inertial sensors," *33rd Annual International Conference of the IEEE EMBS*, pp. 1197–1200, Aug. 2011.

[17] H. J. Luinge, P. H. Veltink, and C. T. M. Baten, "Ambulatory measurement of arm orientation," *Journal of biomechanics*, vol. 40, pp. 78–85, Jan. 2007.

[18] W. H. K. de Vries, H. E. J. Veeger, a. G. Cutti, C. Baten, and F. C. T. van der Helm, "Functionally interpretable local coordinate systems for the upper extremity using inertial & magnetic measurement systems.," *Journal of biomechanics*, vol. 43, pp. 1983–1988, Jul. 2010.

[19] A. G. Cutti, A. Giovanardi, L. Rocchi, A. Davalli, , and R. Sacchetti, "Ambulatory measurement of shoulder and elbow kinematics through inertial and magnetic sensors," *Medical & biological engineering & computing*, vol. 46, pp. 169–178, Feb. 2008.

[20] A. G. Cutti, A. Ferrari, P. Garofalo, M. Raggi, and A. Ferrari, "'Outwalk': a protocol for clinical gait analysis based on inertial and magnetic sensors.," *Medical & biological engineering & computing*, vol. 48, pp. 17–25, Jan. 2010.

[21] M. Ester, H.-p. Kriegel, and X. Xu, "A Density-Based Algorithm for Discovering Clusters in Large Spatial Databases with Noise," *Proceedings of 2nd International Conference on Knowledge Discovery and Data Mining*, pp. 226–231, 1996.